

Computation of transfer maps from magnetic field data in large aspect-ratio apertures

C. E. Mitchell and Alex J. Dragt, University of Maryland, College Park MD, USA

Abstract

Simulations indicate that the dynamic aperture of the proposed ILC Damping Rings is dictated primarily by the nonlinear properties of their wiggler transfer maps. Wiggler transfer maps in turn depend sensitively on fringe-field and high-multipole effects. Therefore it is important to have a detailed and realistic model of the interior magnetic field, including knowledge of high spatial derivatives. Modeling of these derivatives is made difficult by the presence of numerical noise. We describe how such information can be extracted reliably from 3-dimensional magnetic field data $\mathbf{B}(\mathbf{r})$ on a grid as provided by various 3-dimensional finite element field codes, for example OPERA-3d available from Vector Fields. The key ingredients are the use of surface data and the smoothing property of the inverse Laplacian operator. We describe the advantages of fitting on an elliptic cylindrical surface surrounding the beam.

INTRODUCTION

One critical factor in the success of the proposed International Linear Collider will be the design of high-performance damping rings. The damping rings must produce beams with very low emittance while maintaining beam polarization and a sufficiently large acceptance. The dynamic aperture of these damping rings is critically dependent on the quality of the wiggler magnetic field [1]. Often dynamic aperture studies have employed idealized wiggler models [2, 3]. We describe how to obtain a detailed and realistic model of the interior wiggler field, from which realistic transfer maps may be constructed. In particular, we desire a representation for the vector potential that is analytic (so that high derivatives can be computed), satisfies Maxwell's equations exactly, $\nabla \times \nabla \times \mathbf{A} = 0$, and accurately represents the magnetic field.

Expanding about a design orbit through the wiggler at a longitudinal location z yields representations for the components of \mathbf{A} of the (truncated) form

$$A_w(x, y, z) = \sum_{l=1}^L a_l^w(z) P_l(2; x, y). \quad (1)$$

Here $w = x, y$, or z and the $P_l(2; x, y)$ are the various homogeneous monomials in the two transverse deviation variables (x, y) . The deviation variable Hamiltonian H is determined in turn by the Hamiltonian K with z as the independent variable. In Cartesian coordinates, and in the

absence of electric fields, K is given by

$$K = -\left(p_t^2/c^2 - m^2 c^2 - (p_x - qA_x)^2 - (p_y - qA_y)^2\right)^{\frac{1}{2}} - qA_z, \quad (2)$$

and has the (truncated) expansion

$$H = H^2 + H^3 + \dots + H^n = \sum_{s=1}^S h_s(z) P_s(6; x, p_x, y, p_y, \tau, p_\tau). \quad (3)$$

Here the $P_s(6; \dots)$ are the various homogeneous monomials in the six phase-space deviation variables, and the H^m denote the sum of all such terms that are homogeneous of degree m .

Charged-particle motion through the wiggler is described by a symplectic transfer map \mathcal{M} . Through aberrations of order $(n-1)$ such a map has the Lie representation [4, 5]

$$\mathcal{M} = \mathcal{R}_2 \exp(: f_3 :) \exp(: f_4 :) \dots \exp(: f_n :) \quad (4)$$

where \mathcal{R}_2 describes the linear part of the map. The upper limits L and S in the sums (1) and (3) are determined by n . For example, if $n = 6$ then $L = 27$ and $S = 923$.

The linear map \mathcal{R}_2 and the Lie generators f_m are determined by solving the equation of motion $\dot{\mathcal{M}} = \mathcal{M} : -H :$. We conclude that what we need is a Taylor expansion for the vector potential components A_w in the deviation variables x and y . Their z -dependent coefficients $a_l^w(z)$ must be accurately determined from a knowledge of \mathbf{B} .

In general we may have measured or numerical magnetic field data on a discrete mesh of points. The required high derivatives of \mathbf{A} cannot be reliably computed directly from this data by numerical differentiation due to numerical noise whose effect becomes progressively worse with the order of derivative desired. The effect of this noise, and its amplification by numerical differentiation, can be overcome by fitting on a bounding surface far from the axis. We consider, in particular, field data supplied in the domain between pole faces of wiggler magnets with small gap and wide poles (Fig 1). Fitting is done using a cylinder with *elliptical* cross-section. This approach preserves the desirable features of previous approaches that have employed a cylinder with circular cross-section [6], while it improves insensitivity to errors in the boundary data by exploiting the wide pole-face geometry.

As an application, we produced a transfer map for the proposed ILC (CESR-c type) wiggler using data provided

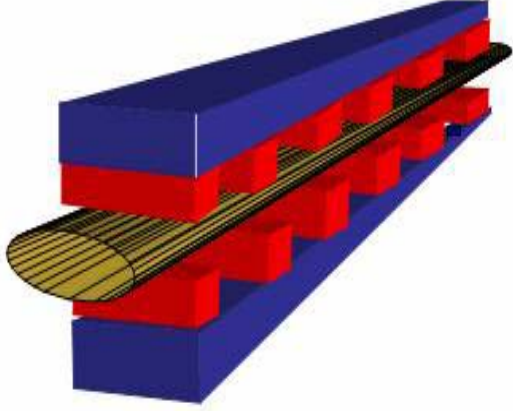


Figure 1: An elliptical cylinder fitting between the pole faces, having large major axis, and extending beyond the fringe-field region.

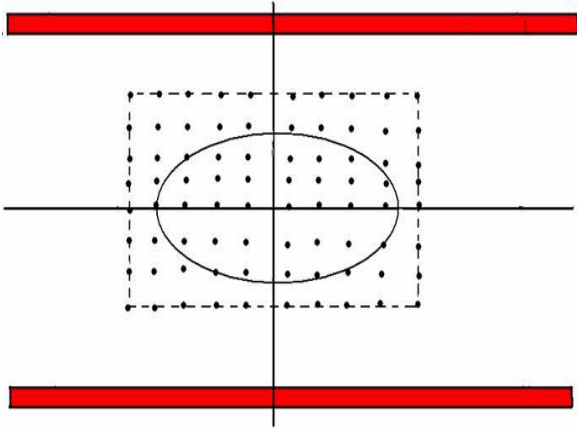


Figure 2: End view of 3-d mesh on which \mathbf{B} is given.

by finite element computations [7, 8]. Values of \mathbf{B} were provided on a rectangular mesh along the full length of the wiggler including the fringe-field regions. The normal component of \mathbf{B} on the surface of an elliptical cylinder was obtained by interpolation using polynomial splines (Fig 2). This normal component on the surface was then used to compute the desired interior expansion (1) for \mathbf{A} using the scalar potential as an intermediate quantity. The normal component of \mathbf{B} on the surface may be written in terms of the scalar potential ψ in elliptic cylindrical coordinates as:

$$\tilde{B}_u(u = U, v, k) = [\partial_u \psi(U, v, k)] / \sqrt{J(U, v)}, \quad (5)$$

$$\begin{aligned} \partial_u \psi(U, v, k) = \\ \sum_{m=1}^{\infty} [F_m(U, k) se_m(v, q) + G_m(U, k) ce_m(v, q)] \end{aligned} \quad (6)$$

Here se_m and ce_m are Mathieu functions [9, 10], $J(u, v)$ is the Jacobian of the mapping from Cartesian to elliptic

coordinates, and $q = -k^2 f^2/4$ where f is the distance of the focus of the ellipse to the axis. All desired quantities may now be written in terms of on-axis gradients $C_{r,s}(z)$, $C_{r,c}(z)$, given by

$$C_{r,\alpha}^{[m]}(z) = \frac{i^m}{2^r r!} \frac{1}{\sqrt{2\pi}} \int_{-\infty}^{\infty} k^{r+m} e^{ikz} \beta_r^\alpha(U, k) dk \quad (7)$$

where

$$\beta_r^s(U, k) = \sum_{m=0}^{\infty} g_s^m(k) B_r^{(m)}(k) \left[\frac{F_m(U, k)}{Se'_m(U, q)} \right], \quad (8)$$

$$\beta_r^c(U, k) = \sum_{m=0}^{\infty} g_c^m(k) A_r^{(m)}(k) \left[\frac{G_m(U, k)}{Ce'_m(U, q)} \right]. \quad (9)$$

Here Se_m and Ce_m are modified Mathieu functions, and the functions g^m , $B_r^{(m)}$, $A_r^{(m)}$ are independent of the geometry or surface data. The key feature of this technique is that results are relatively insensitive to surface errors due to the smoothing property of the inverse Laplacian operator. That is, each kernel multiplying the surface functions F_m and G_m falls off rapidly with frequency k . As a result, high frequency noise in the boundary data has little effect on the functions $C_{r,\alpha}^{[m]}$.

A partial test of the accuracy of this procedure (and on the quality of the magnetic data on the mesh) is that the magnetic field computed from the surface data should reproduce the magnetic field at the interior mesh points. In the case of midplane symmetry, the vertical field through terms of degree four is given in terms of the on-axis gradients (7) by the relation

$$\begin{aligned} B_y = C_1(z) + 3C_3(z)(x^2 - y^2) - C_1^{[2]}(z)(x^2 + 3y^2)/8 \\ + C_1^{[4]}(z)(x^4 + 6x^2y^2 + 5y^4)/192 - C_3^{[2]}(z)(3x^4 \\ + 6x^2y^2 - 5y^4)/16 + C_5(z)(5x^4 - 30x^2y^2 + 5y^4). \end{aligned} \quad (10)$$

There are similar expressions for the other components of \mathbf{B} and the components of \mathbf{A} . (We reiterate that on-axis gradients are obtained using only information about the field on the elliptic cylindrical boundary, and Maxwell's equations are satisfied by construction.) The fit obtained for the vertical field of the proposed ILC wiggler is shown in Fig 3. It employed an elliptical cylinder with semimajor axis 4.4cm and semiminor axis 2.4cm. The field at $x = 0.4$ cm, $y = 0.2$ cm was computed along the length of the wiggler using the Taylor series given in (10). Note in particular the excellent fit to the fringe-fields. Other components of \mathbf{B} are fit equally well. A more demanding test of our procedure has been made by verifying that values for fields and their high derivatives as computed numerically from surface data agree with analytically computed values in the soluble case of fields arising from arrays of magnetic monopoles.

The previous technique can be used effectively for straight-axis magnetic elements. For elements with significant sagitta, such as dipoles with large bending angles, we

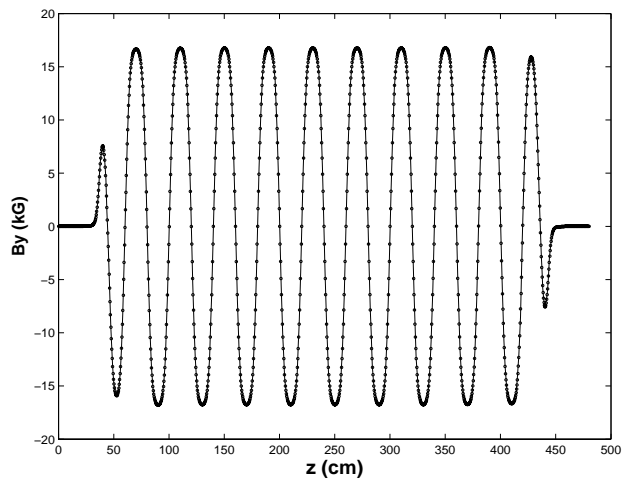


Figure 3: Fit obtained to proposed ILC wiggler vertical field using an ellipse with $x_{max} = 4.4cm$, $y_{max} = 2.4cm$. The solid line is computed from surface data; dots are numerical data provided by OPERA-3d.

must generalize to more complicated domains for which Laplace's equation is no longer separable. Surface data can again be used to fit interior data provided *both* ψ and the normal component of \mathbf{B} are available on the surface. In this case, surface data are integrated against a geometry-independent kernel [11]. Analogous smoothing behavior occurs. We have implemented such a routine for fitting data onto the surface of a bent box. The routine has again been benchmarked using arrays of magnetic monopoles. We verify that $\nabla \cdot \mathbf{B} = 0$ and $\nabla \times \mathbf{B} = 0$ to machine precision, while Taylor coefficients produced were accurate to 10^{-6} .

In summary, surface methods provide a reliable and numerically robust method to extract transfer maps from numerical field data. The smoothing property of the inverse Laplacian operator ensures that computed derivatives are insensitive to errors in the surface data. Such methods provide a promising approach to modeling dynamics in the ILC damping rings and to the general problem of computing realistic transfer maps for real magnets with complicated fringe and high-order multipole error fields.

REFERENCES

- [1] J. Safranek, C. Limborg, et. al., *Nonlinear Dynamics in a SPEAR Wiggler*, Phys. Rev. ST AB **5** (2002) 010701
- [2] J. Gao, *Analytical Estimation of Dynamic Apertures Limited by the Wigglers in Storage Rings*, PAC 2003 p. 3267
- [3] Y. Cai, *Dynamic Aperture in Damping Rings with Realistic Wigglers*, Workshop on Wiggler Optimization for Emittance Control, INFN-LNF (2005)
- [4] A. Dragt and F. Neri, *Lie Algebraic Treatment of Linear and Nonlinear Beam Dynamics*, Ann. Rev. Nucl. Part. Sc. **38** (1988) 455
- [5] A. Dragt, *Lie Methods for Nonlinear Dynamics with Applications to Accelerator Physics*, Draft (2005)

- [6] M. Venturini and A. Dragt, *Accurate Computation of Transfer Maps from Magnetic Field Data*, Nucl. Inst. and Meth. **A427** (1999) 387
- [7] D. Sagan, J.A. Crittenden, D. Rubin, and E. Forest, *A Magnetic Field Model for Wigglers and Undulators*, PAC 2003 p. 1023
- [8] J. Urban, and G. Dugan, *CESR-c Wiggler Studies in the Context of the International Linear Collider Damping Rings*, PAC 2005 p. 1880
- [9] M. Abramowitz, and I. Stegun, *Handbook of Mathematical Functions*, Dover (1972)
- [10] N.W. McLachlan, *Theory and Application of Mathieu Functions*, Dover (1964)
- [11] A.J. Dragt, T.J. Stasevich, and P. Walstrom, *Computation of Charged-Particle Transfer Maps for General Fields and Geometries Using Electromagnetic Boundary-Value Data*, PAC 2001 p. 1776